


# Orebody geometry, fluid and metal sources of the Omitemire Cu deposit in the Ekuja Dome of the Damara Belt in Namibia

Shawn Kitt<sup>1</sup>  · Alexander Kisters<sup>1</sup> · Torsten Vennemann<sup>2</sup> · Nick Steven<sup>3</sup>

Received: 15 September 2016 / Accepted: 23 March 2017  
© Springer-Verlag Berlin Heidelberg 2017

**Abstract** The Omitemire Cu deposit (resource of 137 Mt at 0.54% Cu) in the Ekuja Dome of the Damara Belt in Namibia is hosted by an anastomosing, low-angle Pan-African (ca. 520 Ma) shear zone system developed around an older (ca. 1100–1060 Ma), late Mesoproterozoic intrusive breccia between a suite of mafic rocks (originally lava flows) and later tonalitic gneisses. High-grade ore shoots preferentially formed along contacts between tectonically interleaved biotite-epidote-quartz-chalcocite schists and felsic gneisses, and are directly related to an increase in the number and cumulative thickness of thin, contact-parallel mineralized shear zones. Alteration and mineralization are associated with elevated concentrations of K<sub>2</sub>O, Cr, Rb, S, and Cu and a loss of Na<sub>2</sub>O, CaO, and MgO. Oxygen isotope fractionation for quartz-biotite, quartz-feldspar, and quartz-amphibole mineral pairs support equilibrium temperatures of between 500 and 650 °C during the fluid/rock interaction. Mineral separates from amphibole-biotite gneisses and mineralized schists have similar ranges in  $\delta^{18}\text{O}$  values of about 1.2 to 2 ‰ relative to VSMOW. Coexisting minerals are arranged in an order of

increasing  $\delta^{18}\text{O}$  values from biotite, to epidote, amphibole, and quartz, suggesting that the Omitemire Shear Zone was a rock-dominated system. Similarly, H-isotope results for mineral separates from biotite-epidote schists and amphibole gneisses do not show any reversals for D/H fractionations, with  $\delta\text{D}$  values of between –48 and –82 ‰, typical of metamorphic-magmatic rocks. The homogeneous and low  $\delta^{34}\text{S}$  values (–6.1 to –4.7 ‰ CDT) are compatible with a local redistribution of sulfur from magmatic rocks and interaction with sulfur derived from metamorphic fluids of metasedimentary origin. The relatively low fluid/rock ratios and elevated Cu values (>1500 ppm) from unaltered amphibolite point to a local redistribution of an earlier (late Mesoproterozoic) Keweenaw-type Cu mineralization into later Pan-African shear zones during the exhumation of the Ekuja Dome. The timing, polyphase evolution, and tectonic setting of the Omitemire deposit show remarkable similarities with the large Cu deposits of the Domes Region in the adjoining Lufilian Arc of northern Zambia. This suggests the presence of a much larger, regionally significant Cu province extending from central Namibia, through northern Botswana, and into Zambia.

Editorial handling: H. Frimmel

**Electronic supplementary material** The online version of this article (doi:10.1007/s00126-017-0731-y) contains supplementary material, which is available to authorized users.

✉ Shawn Kitt  
shawnkitt@gmail.com

<sup>1</sup> Department of Earth Sciences, Stellenbosch University, Private Bag XI, Matieland, Stellenbosch 7602, South Africa

<sup>2</sup> Institute of Earth Surface Dynamics, University of Lausanne, Lausanne, Switzerland

<sup>3</sup> Rockwater Consulting, 10 Evergreen Lane, Constantia, Cape Town 7806, South Africa

**Keywords** Damara Belt · Cu · Mesoproterozoic dome · Pan-African · Shear zone · Stable isotopes · Fluid/rock ratio · Lufilian Arc

## Introduction

Central Africa is one of the major Cu provinces in the world. Traditionally, the Central African Copperbelt in the southern Democratic Republic of Congo (DRC) and northwestern Zambia has been known for its sediment-hosted, stratiform Cu deposits (e.g., Selley et al. 2005; Sillitoe et al. 2010;

Hitzman et al. 2012), with possible extensions into the Kalahari Copperbelt of Botswana and Namibia (Borg and Maiden 1989). For the most part, Cu mineralization is hosted by low-grade metamorphic, Neoproterozoic (ca. 880–760 Ma) metasedimentary rocks of the Lower Roan Group in Zambia and the overlying Mines Subgroup in the DRC (Selley et al. 2005; Cailteux et al. 2005; Hitzman et al. 2012). The more recent discoveries of large Cu, U, and Co deposits in the Domes Region in the Pan-African Lufilian Arc of northern Zambia represent a distinct style of Cu mineralization that does not conform to the typical Copperbelt-type mineralization. Instead, Cu mineralization is hosted by high-grade metamorphic, regional-scale domes made up of Meso- and Neoproterozoic basement gneisses surrounded by metasedimentary cover rocks that have a Pan-African tectonic and metamorphic overprint related to the late-stage evolution of convergent and collisional tectonics in the Lufilian Arc (John et al. 2004; Selley et al. 2005; Cailteux et al. 2005; Hitzman et al. 2012). Most studies highlight the high-grade metamorphic wall rock sequence and, in many cases, multiple stages of mineralization, but there is no clear consensus as to the style, controls, and absolute timing of mineralization (Benham et al. 1976; McGowan et al. 2003; Steven and Armstrong 2003; Selley et al. 2005; Bernau et al. 2013; Hitzman et al. 2012; Turlin et al. 2016).

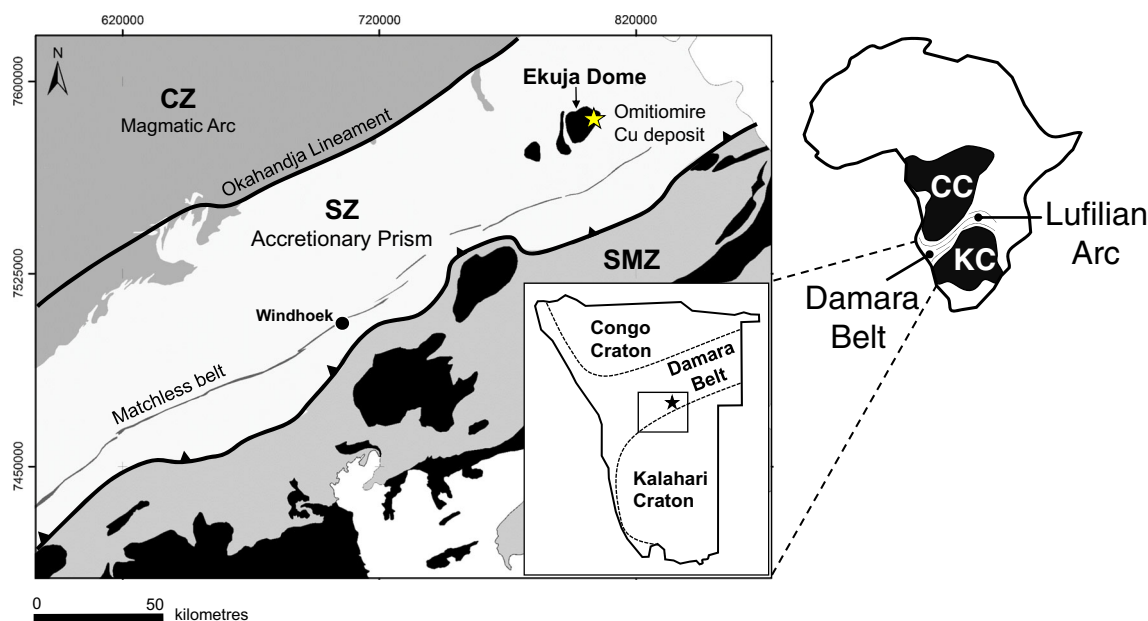
The northeast-trending Damara Belt in Namibia is commonly interpreted to represent the southwestern continuation of the Lufilian Arc (Fig. 1). Both belts have accommodated the amalgamation of the Congo and Kalahari Cratons to form Gondwana in the latest Neoproterozoic and early Phanerozoic (Kampunzu and Cailteux 1999; Miller 1983). The Omitiomire

Cu deposit is hosted by late Mesoproterozoic gneisses and schists that are structurally overlain by amphibolite-facies metasedimentary rocks of the Southern Zone (SZ) accretionary prism (Fig. 1 and electronic supplementary material (ESM) 1). The striking similarities between the Omitiomire deposit and the large Cu deposits in the Domes Region of Zambia suggest similar mineralization processes and controls and an extension of the Cu province from the Domes Region into Namibia (Kitt et al. 2016).

This paper describes the 3D geometry of ore bodies that constitute the Omitiomire deposit, modeled using an extensive drill hole data set. Copper grades and grade envelopes are combined with structural and lithological-geochemical data to describe the internal make up and controls of ore shoots within the deposit. Whole rock geochemical data and mass balance calculations are used to semi-quantitatively characterize element mobility within the mineralized shear zone system. Stable isotope mineral and whole rock data are used to (i) better constrain the temperature conditions of the mineralization and alteration, (ii) constrain fluid/rock ratios during fluid flow, and (iii) discuss the potential source of fluids and metals. Lastly, the deposit-scale data is integrated into the broader geological evolution of the Damara Belt in order to draw possible correlations with seemingly similar styles of mineralization in the Domes Region of the Lufilian Arc in Zambia.

## Geological overview

The Pan-African Damara Belt formed by the high-angle convergence of the Congo and Kalahari Cratons during



**Fig. 1** Simplified geological map (after Miller 2008) showing the location of the Omitiomire Cu deposit relative to the Ekuja Dome and the Southern Zone (SZ) accretionary prism of the Damara Belt of Namibia.

Also shown is the Central Zone (CZ), Southern Margin Zone (SMZ), and locations of the Damara Belt and Lufilian Arc relative to the Congo Craton (CC) and the Kalahari Craton (KC)

the late Neoproterozoic to early Phanerozoic between ca. 580 and 520 Ma (Coward 1981; Miller 1983, 2008; Gray et al. 2008). The Southern Zone (SZ) is the accretionary prism of the belt, developed as a south-verging fold-and-thrust belt that records the off-scraping and burial of the Khomas Sea and thick, trench-fill-type sediments of the Kuiseb Formation during northward subduction below the Congo Craton (Kukla and Stanistreet 1991; Meneghini et al. 2014). The Omitiomire deposit is situated in the Ekuja Dome, one of three gneiss domes at the base of the SZ prism (Fig. 1 and ESM 1). The gneiss domes are made up of late Mesoproterozoic (ca. 1100 Ma) tonalites and amphibolites (Steven et al. 2000) and are structurally overlain by the medium-P, medium-T amphibolite-facies metaturbiditic Kuiseb Formation, and imbricated slivers of serpentinite (Kasch 1986, 1987). Both the structural location and lithological assemblages point to a tectonic position of the gneiss domes close to, or within, the subduction channel, recording initial burial and subsequent expulsion of basement rocks during northward subduction of the Kalahari Craton (Kitt et al. 2016).

## Geology of the Omitiomire deposit

### Host rocks

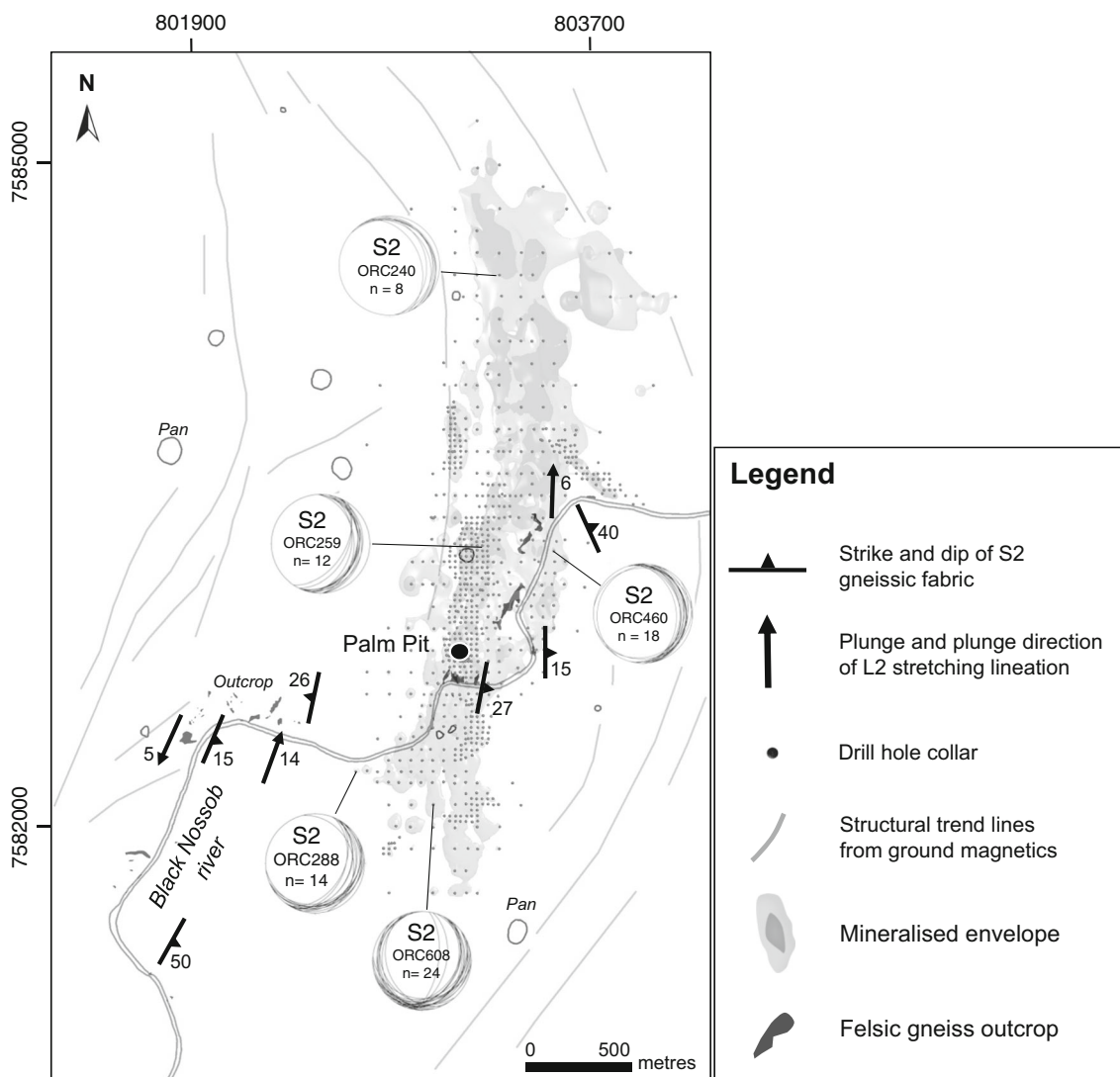
The Omitiomire deposit is situated on the eastern flank of the Ekuja basement dome, close to the structural contact with the overlying Kuiseb Formation of the SZ prism (Fig. 1 and ESM 1). Most of the deposit area is covered by up to 10 m thick, transported Cenozoic (Kalahari) sand, silt, and calcrete. Except for sporadic outcrops in the ephemeral Nossob River and a small sampling pit in the southern part of the deposit, geological information is derived from drill hole data (Fig. 2). The Ekuja Dome is dominated by quartzo-feldspathic banded or augen gneisses of mainly tonalitic composition. The gneisses typically form large sheets and lenses that vary in thickness from a few centimeters up to tens of meters. The tonalitic magma intruded and brecciated a volumetrically subordinate mafic suite of amphibolite. Original intrusive contacts and the brecciation of the older amphibolitic sequence is preserved at lower strain intensities (Kitt et al. 2016) (ESM 2a). At higher strains, angular xenoliths appear progressively sheared out and transposed into the regional gneissic fabrics (S2), associated with the partial or near pervasive retrogression of the rocks (Kitt et al. 2016) (ESM 2b). The intrusive relationship between amphibolite and tonalite is confirmed by U-Pb zircon ages of  $1115 \pm 13$  Ma for amphibolite and  $1084 \pm 7$  and  $1063 \pm 9$  Ma for quartzo-feldspathic gneisses (Steven et al. 2000).

### Structure

Drill core logging and structural mapping of scattered outcrops in the area revealed at least two deformation phases (Kitt et al. 2016). The first phase (D1) in felsic gneisses is defined by the grain-shape preferred orientation of quartz-feldspar aggregates and biotite, and is only observed in the hinges of isoclinal, near recumbent F2 folds that refold the early S1 gneissosity. The second phase (D2) is associated with a regionally developed shallow dipping S2 gneissosity that is parallel to the dome margin and the contact between basement gneisses and overlying Damaran supracrustal rocks. S2 is a well-developed transposition fabric, formed through the progressive refolding of earlier intrusive contacts and the S1 gneissosity by tight to isoclinal F2 folds. This gneissic fabric forms the dominant structural element in the deposit (Steven et al. 2000; Kitt et al. 2016), as well as on a regional scale (Kasch 1987). F2 folds at Omitiomire show north-south trends and subhorizontal northerly or southerly plunges. Fold plunges are parallel to a prominent L2 stretching lineation, defined by rodding fabrics of quartz-feldspar aggregates in gneisses and the preferred alignment of hornblende, plagioclase, and biotite in mafic units along the shallow east-dipping S2 gneissic fabric (Kitt et al. 2016).

### Mineralization

Copper mineralization is spatially associated with variably retrogressed mafic rocks that have formed through the progressive hydration of original amphibolite to amphibole-biotite gneiss and biotite-epidote schist (Steven et al. 2000; Maiden et al. 2013; Kitt et al. 2016). This retrogression is confined to an anastomosing system of mylonitic shear zones, henceforth referred to as the Omitiomire Shear Zone (OSZ). The OSZ is contained in the regional S2 fabric and centered around the lithologically heterogeneous intrusive breccia made up of original amphibolite and tonalite sheets (ESM 2). The Cu resource is largely made up of deeper seated sulfide ore. Shallower oxide-facies ore occurs up to a depth of ca. 40 m below surface and is made up of malachite and subordinate chrysocolla. Chalcocite is the main Cu ore mineral, accounting for more than 90% of sulfide minerals and is texturally intergrown with biotite and epidote. The highest Cu grades are associated with shear bands, veins, and pods that occur in biotite-epidote schists along the lithological contacts with felsic gneisses (Fig. 3a–f) (Kitt et al. 2016). The high-grade biotite-epidote-quartz shear bands are closely associated with either laminated or massive, ribbon-like, and pervasively recrystallized quartz veins or quartz vein relics. Quartz veins are invariably folded or boudinaged, typically forming dismembered boudins and lenses in the biotite-dominated mylonitic shear zones. Large (meter-size) mineralized quartz-biotite-epidote pods or lenses typically occur in the



**Fig. 2** Map of the Omitomire Cu deposit, showing drill hole collars and the subsurface outlines of the orebody. Structural information was compiled from scattered outcrops along the ephemeral black Nossob River, panels along a bulk sample pit (Palm Pit), and data from

downhole photography of drill holes (ORC). Equal area, lower hemisphere stereonet of structural orientation data of the dominant S2 fabric in selected holes are shown. Structural trend lines (light gray) are interpreted from ground magnetic data

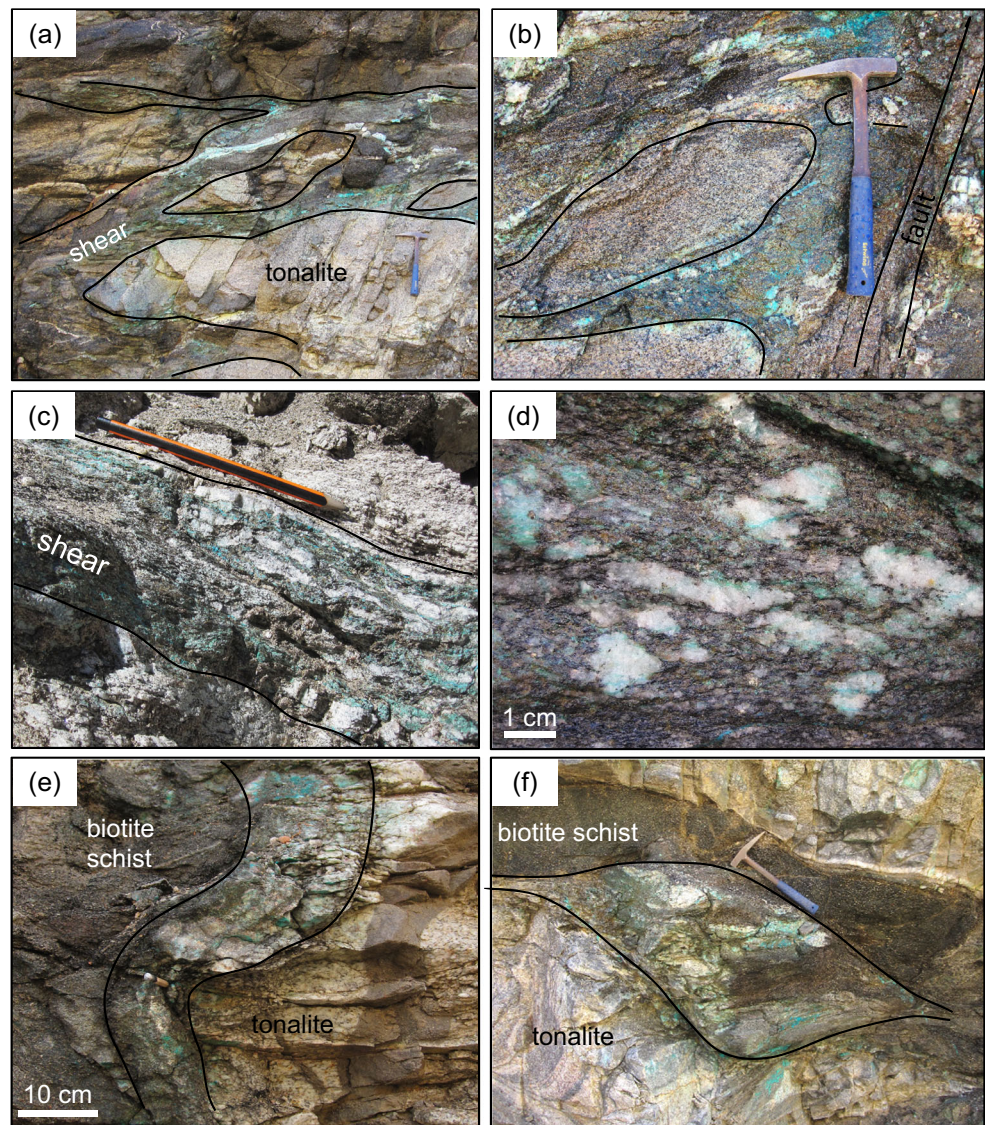
low-strain domains at the contacts between deformed mafic and felsic lenses and are stretched in a north-south direction. Details of the structural controls and evolution of the Cu mineralization have been presented in Kitt et al. (2016).

### 3D implicit modeling

The visualization and description of the geometry of the subsurface geology and distribution of Cu mineralization relied on the 3D modeling of an extensive drill hole dataset, including geological, structural, and assay data from roughly 100 km of drilling (Figs. 2 and 4). The modeling was carried out using Leapfrog Geo 3D modeling software and an implicit modeling approach with drill hole data in a volume of 4 km in a north-

south direction, 2 km from east to west, and up to 800 m below the surface (Fig. 4). Due to the structural and lithological complexity and relatively wide spacing of drill holes in some areas, a meaningful lithological model of the OSZ was only possible through the definition of wider and, in places, heterogeneous rock packages, without compromising the integrity of the data and losing necessary detail (Fig. 4a). For example, smaller, meter-wide sheets of felsic gneiss intercalated with mainly biotite-epidote and amphibole-biotite gneiss units were grouped together into the mafic-dominated unit. Similarly, meter-scale amphibolite and mafic schist bodies may appear as isolated and seemingly discontinuous units in otherwise felsic gneisses. These isolated and discontinuous amphibolite bodies probably formed rafts intruded and dismembered by tonalitic magma similar to the intrusive relationships developed

**Fig. 3** Photographs of the main types of high-grade mineralization described in the Palm Pit at Omitimire. **a** Mineralized biotite-epidote-quartz shears in biotite-epidote schist. Note rafts of tonalite enveloped by the shear zones. **b** Close-up of shears and tonalite rafts. **c** Mineralized quartz-biotite-epidote shear containing dismembered and boudinaged quartz veins and vein relics. **d** Close-up of shear zone showing patch-like stretched relics of milky quartz in a matrix of biotite, epidote, quartz, and malachite. **e** Steeply dipping folded, laminated quartz vein along the contact between biotite schist and tonalite. The vein selvage is made up of biotite, epidote, and malachite. **f** Large quartz-biotite-epidote-malachite pod in a strain shadow at the contact between biotite schist and tonalite



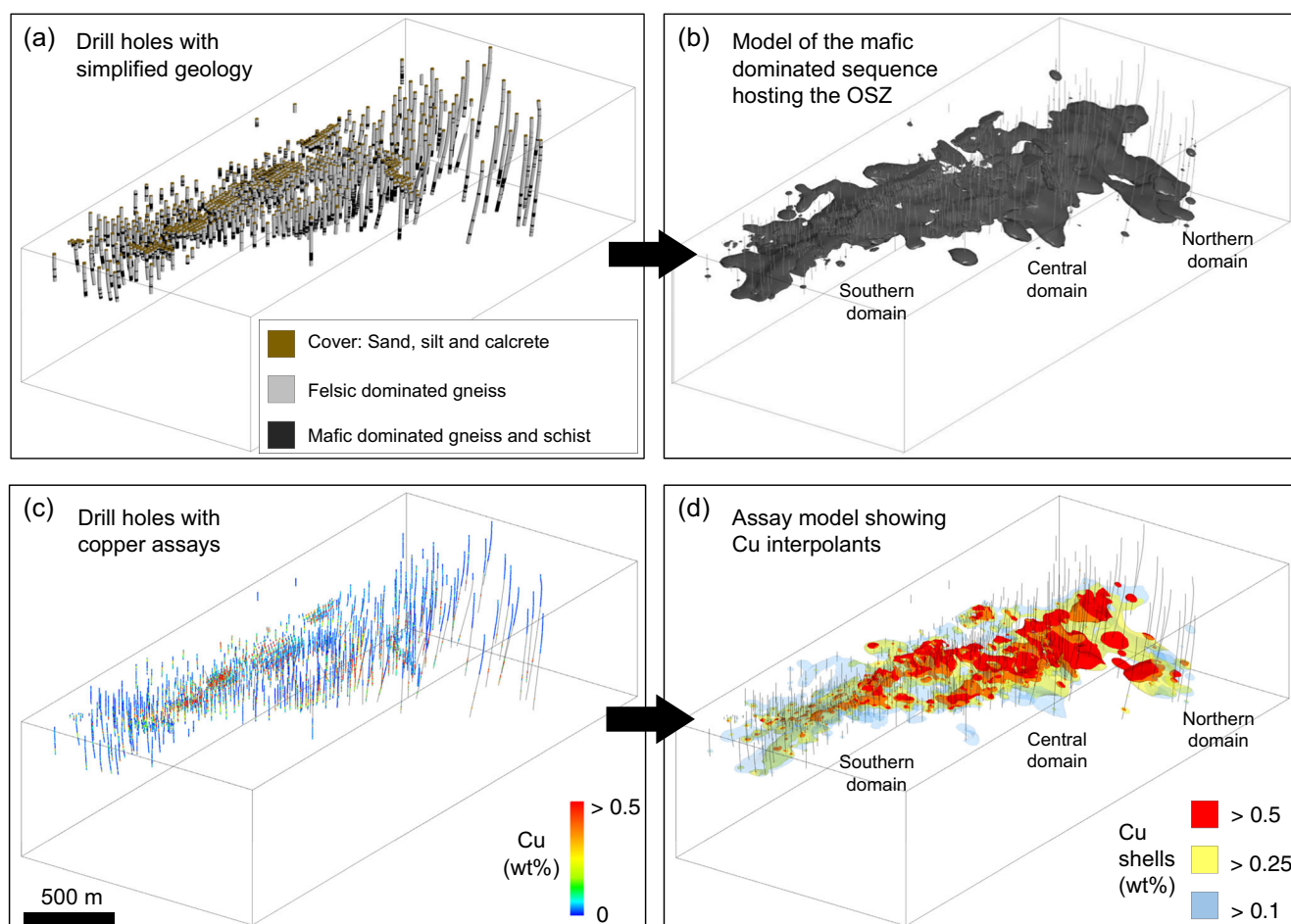
in the southern sampling pit where amphibolite and tonalite formed an original intrusive breccia (Kitt et al. 2016). In the deposit-scale model, these small, isolated mafic units in the wall rocks were grouped together with the felsic gneisses (Fig. 4b).

For the assay model, some 80,139 Cu assays from 1 m sampling intervals from drill holes were processed and isotropic grade shells with cut-off grades of 0.1, 0.25, and 0.5 wt% Cu were created (Fig. 4c, d). A structural trend was created from structural data generated from downhole photography of drill holes and applied to the model. For descriptive purposes, the model was divided into northern, central, and southern domains.

### 3D model of the OSZ host rocks

The lithological model shows a central, gently undulating, shallowly east-dipping sequence dominated by biotite-epidote schists and amphibole-biotite gneisses (Figs. 4b and 5). This central unit is enveloped by mainly quartzo-feldspathic gneisses

with only minor lenticular pods of biotite schist, amphibole gneiss, and/or interlayered banded mafic and felsic gneisses. Tight to isoclinal folds (F2) affected the interlayered gneisses and result in the large-scale transposition of structures and fabrics. Mylonitic fabrics are common, particularly in mafic schists and along lithological contacts between felsic gneisses and mafic schists. On a deposit scale, the 3D model indicates the presence of several tens of meters-thick lenses that pinch and swell and coalesce to form a large up to 100 m thick sequence of dominantly mafic gneisses and schists (Fig. 5). Individual mafic lenses are separated by sheet-like tonalitic gneisses and/or interlayered mafic-felsic gneisses and schists that vary in thickness from a few meters to several tens of meters. This central mafic unit is contained in the regional S2 fabric, evident from structural data generated from downhole photography and surface mapping (Figs. 2 and 5). It shows easterly dips, but with gentle undulations from moderately east dips (30°) in the northern domain, to shallowly east (15°) in the central domain, to



**Fig. 4** Simplified workflow for the 3D implicit modeling of the Omitiomire deposit. **a** Geological drill hole logging data, simplified with the interval selection tool in Leapfrog Geo. **b** Lithological model (with structural trend applied) of the mafic gneiss and schist-dominated

subhorizontal and shallowly ( $20^\circ$ ) westerly dips in the southern domain (Fig. 5). These variations describe an open arcuate geometry.

### 3D model of Cu assays

Potentially economic-grade ( $>0.25$  wt% Cu) mineralization is confined to a gently undulating, overall tabular, arcuate zone that dips between  $20^\circ$  and  $30^\circ$  to the east. The overall deposit-scale geometry of the orebody resembles an asymmetric upward-curved lens with a long axis that strikes for more than 4 km in a north-south direction (Fig. 6a–c). The deepest part of the deposit occurs in the northern domain where the mineralization continues beyond 600 m below surface (Figs. 5 and 6b). Although largely covered by sand, silt, and calcrete, the orebody is at the surface in the western parts of the central domain (Fig. 6c). In the southern domain, the orebody is characterized by westerly and ESE dips and by a shallow plunge to the south (Fig. 6c). Both the down-dip and strike extent of the mineralization remain open. Current information suggests that there are no

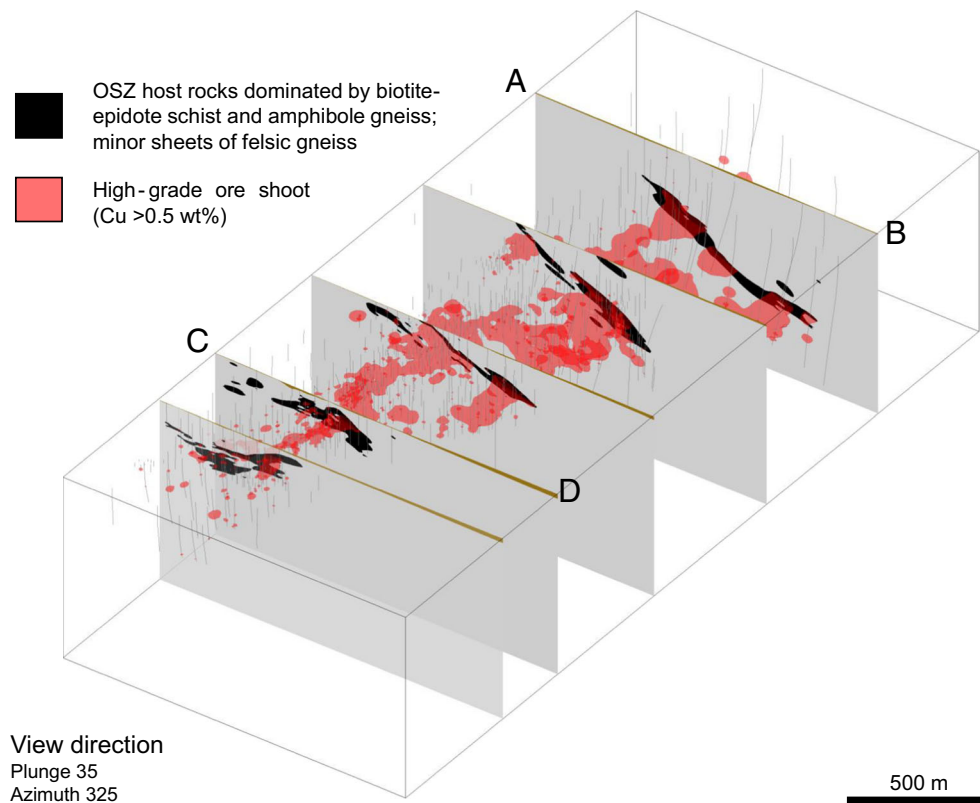
sequence that host the Omitiomire deposit. **c** Drill hole traces showing Cu assays at 1 m sampling intervals. **d** Assay model showing Cu  $>0.5$  wt%, Cu  $>0.25$  wt%, and Cu  $>0.1$  wt% interpolants with structural trend applied. The plunge and azimuth of the view direction is  $25^\circ$  and  $325^\circ$

obvious late faults or major structural breaks that offset the mineralization.

### Internal architecture and controls of high-grade ore shoots

The highest Cu grades generally occur in the upper parts of the main mineralized envelope along the hanging wall (HW) contact with the overlying felsic-dominated HW gneiss. The high-grade ore envelope is defined by  $>0.5$  wt% Cu that forms a distinct lens-like shoot, composed of an up to 100 m thick central part based on current drill hole information (Fig. 6). The high-grade ore envelope also delineates zones of thickened high-grade mineralization that define two distinctly linear north-south trending ore shoots, here referred to as OS1 and OS2 (Fig. 6a–c). The gently undulating ore shoots are characterized by north-south to NNE strikes and shallow plunges to the north and south, parallel to the regional stretching lineation (L2). In cross section, both shoots have typical stacked

**Fig. 5** Serial cross sections through the deposit showing the simplified lithological model and unsliced high-grade mineralized shell (Cu > 0.5 wt%). The locations of sections A, B and C, D presented in ESM 3 are shown



lens geometries and an associated thickening of the mafic-dominated host rock sequence (ESM 3). Copper mineralization correlates with intercepts of biotite-epidote schist, with the highest Cu grades closely associated with the contacts of larger mafic schist packages against quartzo-feldspathic gneisses or within intercalated schist-gneiss packages (ESM 3 and Fig. 7). This is the case not only for individual schist intersections but also for the ore lens as a whole. High-grade shoots are directly related to the occurrence of biotite-epidote-quartz shear bands and centimeter-scale quartz veins with mineralized selvages in biotite-epidote schists (Fig. 7). Individual veins and shear bands are only 1–10 cm wide, but form part of a wider system of anastomosing mineralized shears where individual shears are tightly spaced. The shears and veins developed along the contacts of biotite-epidote schists against the felsic gneisses and high-grade ore shoots are directly related to an increase in the frequency of contact-parallel shears and veins (Fig. 7). This underlines the combined effects of the structural and lithological controls on Cu mineralization at Omitiomire (Kitt et al. 2016).

## Hydrothermal alteration and mass balance

### Petrography

The progressive replacement of original hornblende-plagioclase assemblages by hornblende-biotite and biotite-

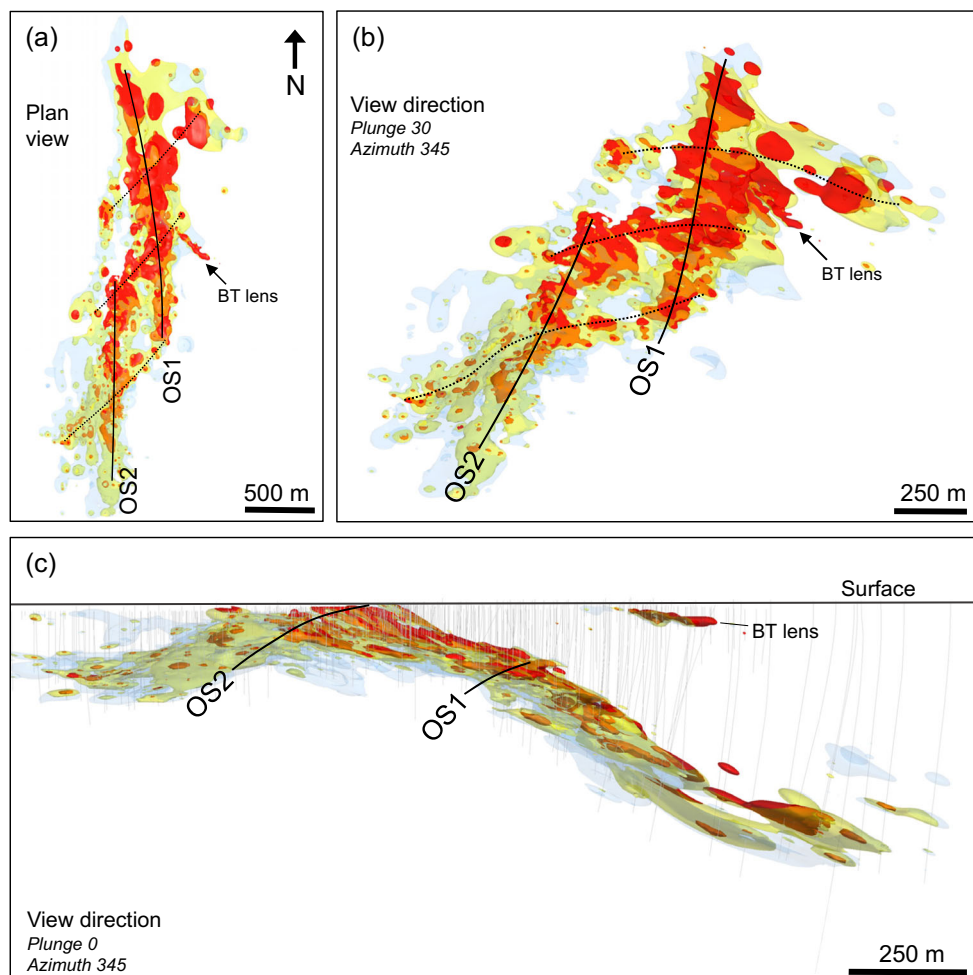
epidote assemblages in schists from within the OSZ suggests variable hydration and retrogression of original amphibolites during deformation and accompanying fluid flow (Steven et al. 2000; Kitt et al. 2016; Fig. 8).

Unaltered and unretrogressed amphibolites of the original wall rock sequence are dominated by hornblende and plagioclase that constitute up to 80 vol% of the rock. Quartz (<10 vol%), biotite (<5 vol%), titanite, rutile, ilmenite, and garnet occur in variable amounts, but rarely exceed more than a few percent. Compositional variations are indicated by different relative abundances of hornblende and plagioclase, distinguishing more melanocratic from relatively leucocratic varieties. Texturally, the amphibolites are granoblastic, massive to foliated or, more commonly, lineated, marked by the preferred alignment of aggregates of hornblende and plagioclase.

The hornblende-biotite gneisses are characterized by relics of hornblende that are progressively replaced and enveloped by S2-parallel aggregates of biotite that can constitute up to 30 vol% of the gneisses. Biotite is associated with small epidote porphyroblasts and minor amounts of disseminated chalcocite.

Biotite-epidote schists result from the near-complete replacement of original amphibolite and are made up of >50 vol% biotite, >15 vol% epidote, 10–20 vol% quartz and plagioclase, 5–10 vol% hornblende, 1–5 vol% chalcocite, and minor amounts of titanite, chlorite, apatite, and rutile. The biotite occurs as sheet-like aggregates that are wrapped around large porphyroblasts of epidote and relic hornblende/plagioclase, thus forming a strong anastomosing S2 fabric.

**Fig. 6** Assay model of the deposit. High-grade ( $\text{Cu} > 0.5 \text{ wt}\%$ ) shoots are in *red*, surrounded by lower grade  $\text{Cu} > 0.25 \text{ wt}\%$  in *yellow* and  $\text{Cu} > 0.1 \text{ wt}\%$  in *light blue*. **a** Plan view showing the north-south trend of high-grade shoots OS1 and OS2 and interpreted subordinate NE mineralized trends. **b** Oblique view to the NE, showing the high-grade shoots OS1 and OS2 and interpreted subordinate NE mineralized trends. **c** Unsliced cross section with view to the NE illustrating the upward convex lens shape of the orebody. The location of high-grade ore shoots OS1 and OS2 along the L2/S2 fabric and the disconnected BT lens in the hanging wall are shown



## Mass balance

Chemical variations (e.g., enrichments and depletions) and volume change related to fluid/rock interaction during deformation and hydrothermal alteration can be quantitatively estimated by applying the isocon method (Grant 1986) to the bulk geochemistry of variably altered and unaltered samples. This approach is based on the theory of Gresens (1967) and has since been widely applied to studies of element mobility in shear zones (O'Hara 1988; Goddard and Evans 1995; Hippertt 1998; Streit and Cox 1998; Zulauf et al. 1999; Rolland et al. 2003; Barnes et al. 2004) and hydrothermal ore deposits (Gregory 2006; Fisher et al. 2013; Oliver et al. 2015).

## Results

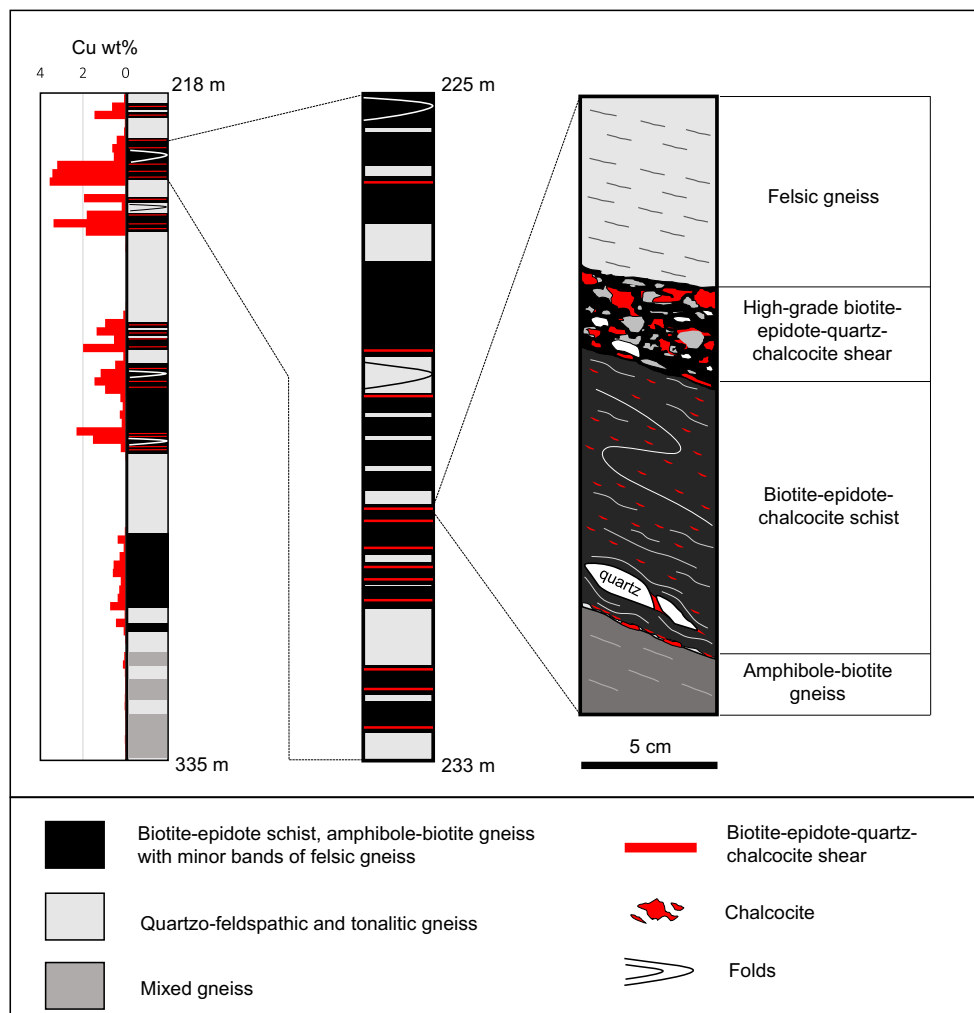
### Element mobility

The whole rock XRF and ICP data of variably altered and mineralized drill core samples from the Omitiomire deposit

were plotted against those of an unaltered sample collected some 7 km away from the deposit in order to compare the elemental gains and losses during alteration and mineralization (Fig. 9 and table in ESM 4). The altered samples include hornblende-plagioclase gneiss and biotite-epidote-chalcoite schist from high-grade shear zones in the deposit (Fig. 8). The element concentrations of the sample types were averaged and arbitrarily scaled for visualization purposes before plotting. Only elements deemed most important during the retrogression of amphibolite to biotite-epidote schist, as described above, are presented. Where possible, the isocon line has been chosen based on the linear correlation of as many elements as possible. Attempts were made to include immobile elements such as Al and Ti. However, some of the supposedly immobile elements were evidently slightly mobile during alteration and mineralization in some of the samples.

Figure 9a shows the average of analytical data from two weakly altered hornblende-plagioclase gneiss samples from the OSZ plotted against the average of two regional and unaltered amphibolite samples. Although none of the conventional





**Fig. 7** Simplified geological log of drill core from a hole that intercepted the north-south trending high-grade shoot OS1 in the northern domain (sections A-B) of the Omitomire deposit (Fig. 5 and ESM 3). The figure illustrates the association of high-grade Cu mineralization with the intercepts of centimeter-scale quartz-biotite-epidote-chalcocite shears and veins (in red) in units of biotite-epidote schist and amphibole gneiss (in black) close to the contacts with felsic gneisses. In the figure, OS1 is composed of an upper and lower lens of high-grade mineralization that is hosted by several closely spaced sheets of biotite-epidote schist and

separated by a large 10 m thick lens of tonalitic gneiss. The upper lens is about 20 m thick and contained in 1–5 m thick sheets of biotite-epidote schist. The lower lens is about 22 m thick and hosted by sheets of biotite-epidote schist that vary in thickness from 1 to 12 m. In the upper lens, more than 12 high-grade biotite-epidote-quartz shears and veins were counted over a distance of 8 m, and up to 10 shears and veins over 22 m in the lower lens. On a deposit scale, high-grade shoots are directly related to the occurrence and cumulative thickness of the thin, mineralized shears and veins

immobile elements plot directly on a straight line, a best fit isocon can be fitted through Ti and Al. Elements such as Ce, Fe, and Zr also plot close to the isocon, which may suggest limited mobility. For this case, the isocon diagram indicates a depletion of CaO, MgO, and Zn and a slight enrichment in K<sub>2</sub>O, Rb, Th, P<sub>2</sub>O<sub>5</sub>, Pb, and Cu.

Figure 9b plots the average analytical compositions from two mineralized biotite-epidote schists from high-grade shear zones in the OSZ against the average of the unaltered amphibolite samples. Although the diagram shows a much larger scatter of elements, an isocon was again selected based on a line of best fit through Al and Ti. The isocon diagram indicates a significant depletion of Na<sub>2</sub>O, CaO, and to some extent MgO. In contrast, K<sub>2</sub>O,


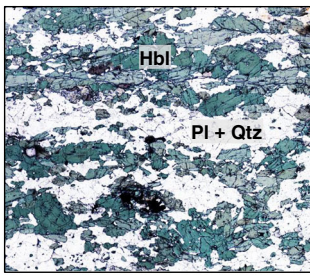
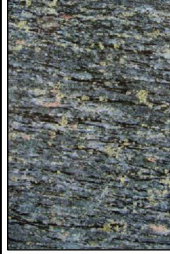
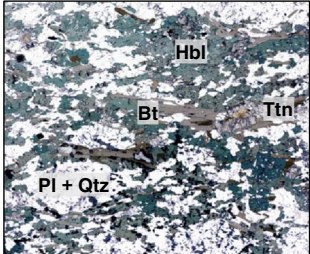
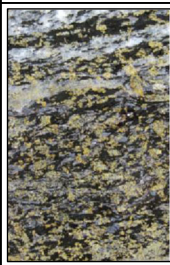
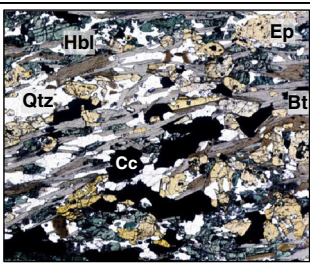
Cu, Cr, Rb, S, and, to a lesser extent, Th, U, Pb, Ni, Fe, and Zn are markedly enriched in the schist relative to the country rocks.

### Stable isotope compositions

#### Samples and analytical methods

Stable O- and H-isotope compositions of mineral separates from amphibole gneisses, biotite-epidote schists, and associated quartz veins in the deposit were used to constrain the likely fluid sources, fluid/rock ratios, and the conditions

**Fig. 8** Drill core photos and photomicrographs showing the main mineral assemblages associated with the progressive replacement of original hornblende-plagioclase assemblages by hornblende-biotite and biotite-epidote paragenesis in the Omitomire Shear Zone

Sample Description	Drill core	Thin Section	Mineral Assemblage
	2 cm	1 cm	
Hornblende-plagioclase gneiss			Hornblende (Hbl), plagioclase (Pl), quartz (Qtz), minor biotite (Bt)
Hornblende-biotite gneiss			Hornblende, plagioclase, quartz, biotite, epidote (Ep) and minor titanite (Ttn)
Biotite-epidote schist			Biotite, epidote, quartz and plagioclase, hornblende, chalcocite (Cc) and minor titanite

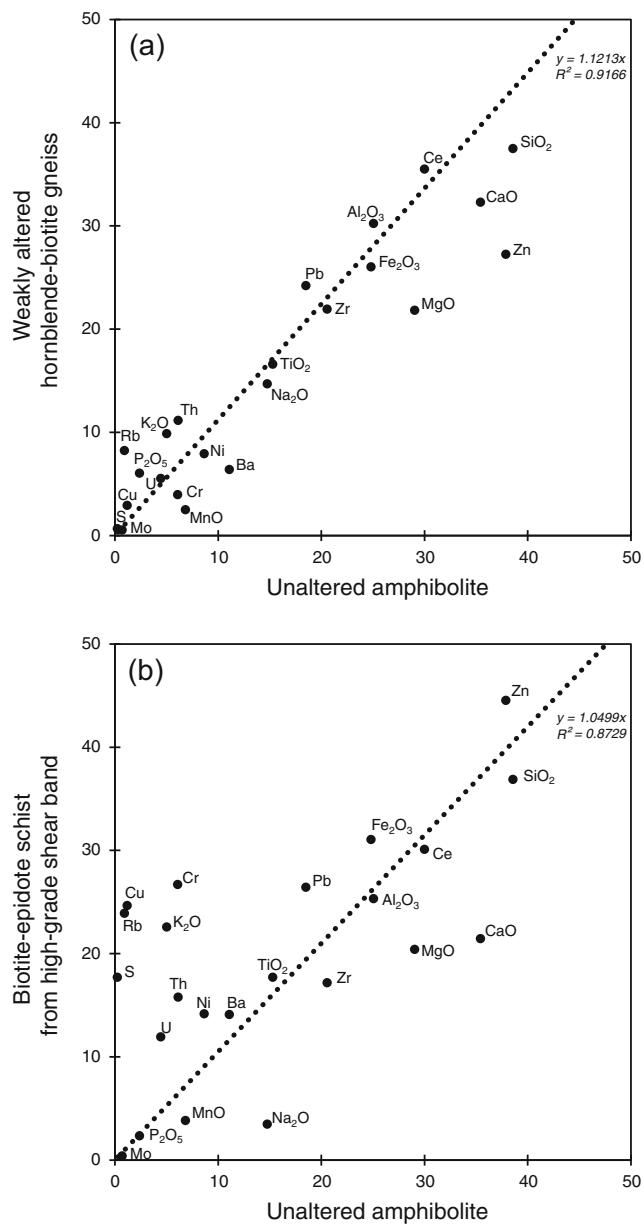
during deformation and Cu mineralization in the mineralized OSZ.

The oxygen isotope compositions ( $^{16}\text{O}$ ,  $^{18}\text{O}$ ) were measured at the University of Lausanne, using a method similar to that first described by Sharp (1990) and in more detail in Vennemann et al. (2001). Between 0.5 and 2 mg of sample was loaded onto a small Pt-sample holder and pumped out to a vacuum of about  $10^{-6}$  mbar. After pre-flourination of the sample chamber overnight, the samples were heated with a  $\text{CO}_2$  laser in 50 mbar of pure  $\text{F}_2$ . Excess  $\text{F}_2$  was separated from the  $\text{O}_2$  produced by conversion to  $\text{Cl}_2$  using KCl held at 150 °C. The extracted  $\text{O}_2$  was collected on a molecular sieve (13X) and subsequently expanded into the inlet of a Thermo-Finnigan MAT 253 isotope ratio mass spectrometer. Oxygen isotope compositions are given in the standard  $\delta$ -notation, expressed relative to VSMOW in per mill (‰). Replicate oxygen isotope analyses of the standard used (NBS-28 quartz;  $n = 12$ ) has an average precision of  $\pm 0.1$  ‰ for  $\delta^{18}\text{O}$ . The accuracy of  $\delta^{18}\text{O}$  values is better than 0.2 ‰ compared to accepted  $\delta^{18}\text{O}$  values for NBS-28 of 9.64 ‰.

Measurements of the hydrogen isotope compositions of minerals were made using high-temperature (1450 °C)

reduction methods with He-carrier gas and a TC-EA linked to a Delta Plus XL mass spectrometer (Thermo-Finnigan) on 2 to 4 mg-sized samples according to a method adapted from Sharp et al. (2001) and described in more detail in Bauer and Vennemann (2014). The results are given in the standard  $\delta$ -notation, expressed relative to VSMOW in per mill (‰). The precision of the in-house kaolinite and G1 biotite standards for hydrogen isotope analyses was better than 2 ‰ for the method used; all values were normalized using a value of  $-125$  ‰ for the kaolinite standard and  $-65$  ‰ for NBS-30.

The S-isotope compositions were measured in the Stable Isotope Laboratory of the University of Lausanne using a Carlo Erba (CE 1100) Elemental Analyzer linked to a ThermoFisher Delta V mass spectrometer. Samples were reacted at 1050 °C in a stream of He-carrier gas spiked with oxygen gas. The isotopic composition is expressed in the conventional  $\delta$ -notation ( $\delta^{34}\text{S}$ ) relative to V-CDT in parts per thousand (per mill). External reproducibility of standards and samples (all analyzed twice) is better than 0.15 ‰ and samples were calibrated against IAEA standards S1 and S3 ( $\text{Ag}_2\text{S}$ ) and NBS-127 ( $\text{ZnS}$ ) with accepted values of  $-0.3$ ,  $-32.1$ , and 20.3 ‰, respectively.



**Fig. 9** Isocon diagrams of average element concentrations in unaltered amphibolite plotted against **a** weakly altered hornblende-biotite gneisses and **b** biotite-epidote schists from high-grade shear bands in the Omitiomire deposit. The isocon is defined by the linear correlation and relative immobility of  $\text{TiO}_2$  and  $\text{Al}_2\text{O}_3$ . Elements that plot above the isocon were gained; elements below were depleted. The data was scaled for visualization purposes

## Results

### Oxygen isotope compositions

All stable isotope compositions are reported in a table in ESM 5. Quartz separates from quartz veins as well as separates from biotite-epidote-chalcocite schists have  $\delta^{18}\text{O}$  values between 9.3 and 10.1 ‰. Similarly, the

oxygen isotopic composition of quartz from amphibole-biotite gneisses and thin biotite-rich layers in banded felsic gneisses have values between 8.9 to 9.8 and 8.9 to 9.9 ‰, respectively. The  $\delta^{18}\text{O}$  values of epidote and biotite from amphibole-biotite gneisses and biotite-epidote schists have a range between 5.2 and 6.4 and 3.2 and 5.0 ‰, respectively. Amphibole separates from partially retrogressed amphibole-biotite gneisses and schists have  $\delta^{18}\text{O}$  values between 4.1 and 6.1 ‰. The mean value of  $\delta^{18}\text{O}_{\text{amp}}$  in the gneisses is 5.8 ‰, somewhat higher than the mean of 4.6 ‰ of  $\delta^{18}\text{O}_{\text{amp}}$  in the schists. The  $\delta^{18}\text{O}$  values of feldspar from ore zone schists and gneisses are 9.8 and 7.5 ‰, respectively, while single chlorite and fuchsite separates have  $\delta^{18}\text{O}$  values of 5.3 and 6.5 ‰. Hence, all minerals have similar ranges in their  $\delta^{18}\text{O}$  values of about 1.2 to 2 ‰. This range is similar to the range in values measured for a sequence of whole rocks associated to the mineralization at Omitiomire (between 6 and 7.8 ‰). Furthermore, the coexisting minerals are arranged in an order of increasing  $\delta^{18}\text{O}$  values from biotite, to epidote, amphibole, and quartz, as would be predicted from the theory of stable isotope fractionation between minerals (e.g., Hoefs 2009). Apparent temperatures of equilibration calculated for quartz-biotite and also quartz-amphibole O-isotope fractionations (based on fractionation factors after Bottinga and Javoy (1975) and/or theoretical fractionation factors based on Zheng (1995)) also have a small range of between 490 to 620 and 520 to 660 °C, respectively (ESM 5), values that are consistent with the regional grade of metamorphism (Kasch 1987).

### Hydrogen isotope compositions

Hydrogen isotope compositions of hydrous minerals from the mineralized biotite-epidote schists and amphibole-biotite gneisses have a range of  $\delta\text{D}$  values between  $-48$  and  $-82$  ‰ (ESM 5). The  $\delta\text{D}$  values for biotite in all samples are between  $-58$  and  $-82$  ‰ and for amphibole between  $-66$  and  $-79$  ‰. Biotite-epidote schists ( $-58$  to  $-70$  ‰) have somewhat lower  $\delta\text{D}_{\text{bt}}$  values compared to the amphibole gneisses ( $-68$  to  $-82$  ‰) and felsic gneisses ( $-62$  to  $-80$  ‰), but the range in values does overlap to a large extent. Single fuchsite and chlorite separates have  $\delta\text{D}$  values of  $-48$  and  $-60$  ‰, respectively.

### Sulfur isotope compositions

Only chalcocite separated from veins, whole rocks, and contact zones between different rock types was analyzed for its sulfur isotope composition (ESM 6). The values are remarkably homogeneous, irrespective of the location of the chalcocite (vein, pegmatite, whole rock matrix, contact zone), with an average of  $-5.4$  ‰ ( $\pm 0.45$  ‰ at  $1\sigma$ ;  $n = 13$ ).

## Discussion

### Fluid flow and development of the OSZ

The controls and petrographic characteristics of the Omitomire Cu mineralization have recently been described by Kitt et al. (2016). In that study, it was established that Cu mineralization and fluid flow were structurally controlled and related to Pan-African, D2 deformation. The Pan-African timing of deformation is also indicated by U-Pb titanite ages of 520–485 Ma in the mineralized biotite-epidote schist (Steven et al. 2000; Maiden et al. 2013). Fluid flow was controlled by transient fracture permeability particularly along lithological contacts between original amphibolite and tonalite within and along the late Mesoproterozoic (ca. 1100–1060 Ma) intrusive breccia in gneisses of the Ekuja Dome. Initial veining and fluid flow were confined to the marginal zones of competent amphibolite xenoliths. The progressive retrogression of the rocks, notably of the mafic lithologies to biotite-dominated schists led to further strain localization, particularly along biotite-epidote schists that have formed along contacts between mafic xenoliths and quartzo-feldspathic gneisses (Kitt et al. 2016). This reaction softening accounts for the spatial relationship between mylonitic and highly transposed fabrics of the central OSZ system localized around the originally heterogeneous intrusive breccia (Kitt et al. 2016).

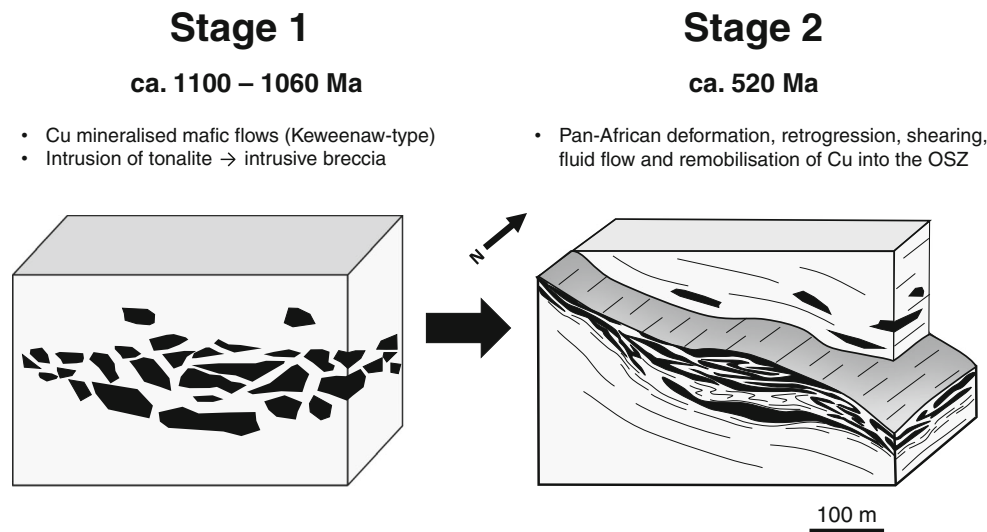
These detailed controls of fluid flow and mineralization find their manifestation in the deposit-scale controls of Cu mineralization and ore shoots. The detailed logging and sampling combined with the deposit-scale modeling indicates that potentially economic-grade Cu mineralization is not necessarily associated with thick intersections of relatively massive mafic rocks in the OSZ. Instead, the highest Cu grades are developed in intervals of closely interlayered mafic schist and felsic gneiss units and particularly along the upper contacts of schist units against gneisses. High Cu grades are commonly confined to narrow, contact-parallel shears along contacts between mafic units against surrounding gneisses (Fig. 7). The actual thickness of high-grade lenses or shoots is determined by the number and cumulative thickness of the thin, mineralized shear zones. This underlines the role of original wall rock heterogeneity for the structurally controlled fluid flow and mineralization. The distribution of wall rock heterogeneities and, thus, the occurrence of high-grade lenses and shoots are determined by the interaction and superimposition of the original geometry and extent of the late Mesoproterozoic intrusive breccia, and later Pan-African strains (D2), recorded by transposition folding, the duplication, and also attenuation of mafic units (Fig. 10). The strain localization into the central mafic schist unit is likely to have modified the original geometry of the intrusive breccia and original intrusive relationships. Notably, the ore shoots trend

north-south, parallel to the regional stretch (L2) and are contained within the undulating high-strain S2 foliation (Fig. 6). This implies that the geometry and orientation of ore shoots or lenses in the OSZ and at higher finite strains are determined by D2 strains. The development of the OSZ as a regionally significant shear zone system able to channel regional-scale fluid flow probably hinged on the presence and distribution of closely spaced, albeit irregularly distributed mafic xenoliths in the central parts of the intrusive breccia. This may explain the lack of mineralization in isolated mafic xenoliths outside the central OSZ, mainly located in the hanging wall of the anastomosing shear zone and, thus, bypassed by the main fluid plumbing system. A localized mineralized lens (BT lens in Fig. 6c) in the HW of the main mineralization may represent the incipient case of shear zone formation. In this case, a cluster of mafic rocks resulted in strain localization and localized shearing, but without developing into a laterally more extensive shear zone system. This highlights the potentially very patchy geometry of the mineralization for the broader Ekuja Dome that reflects the combined effects of the original late Mesoproterozoic (about 1100 Ma) geometry of the intrusive breccia between amphibolite and tonalitic gneisses, overprinted and modified by later Pan-African strains that determined fluid flow in the shear zone system (Fig. 10).

### Mass transfer during fluid flow

Petrographic studies and the chemical analysis of variably retrogressed samples from the OSZ provide a record of the chemical exchange that took place during deformation and fluid flow. The isocon method used here is not without problems since typically immobile elements have evidently been mobile, so that the mass balance diagrams may indicate trends of element mobility, but absolute values of element mobility have to be viewed with caution.

The mass balance diagrams document that the hydration of amphibolites to biotite-epidote schists in the OSZ is consistently associated with significant increases in Cu, Cr, Rb, S, and K<sub>2</sub>O (Fig. 9). The increased K<sub>2</sub>O and Rb contents during alteration and mineralization are reflected by the formation of biotite in biotite-epidote schists that host the mineralization (Fig. 8). Significant enrichments in Cr correlate with the Cu mineralization and Cr-epidote in the biotite-epidote alteration assemblage and, to a lesser extent, Cr-rich magnetite (Steven et al. 2000). The enrichment of the mineralized parts of the OSZ in Cr clearly points to the solubility of Cr in the mineralizing fluid. A potential source for Cr may be found in the alteration of originally ultramafic rocks to serpentinites that occur in abundance as structurally interleaved slivers at the top of the Ekuja Dome and with the structurally overlying Kuiseb Formation metaturbidites (ESM 1). The structurally imbricated serpentinite bodies underline the position of the



**Fig. 10** Conceptual model illustrating the main stages for the development of the Omitomire Cu deposit. *Stage 1* Late Mesoproterozoic (ca. 1100 Ma) basaltic rocks (originally lava flows) with Cu mineralization (Keweenaw-type) were intruded by voluminous tonalitic magma (ca. 1060 Ma) to form an intrusive breccia consisting of xenoliths of basalt in the tonalite. *Stage 2* Pan-African (ca. 520 Ma) deformation and hydration resulted in the retrogression of amphibolites

to biotite-epidote schists, strain localization, fluid flow, and remobilization of Cu into mylonitic shear zones that formed in the schists. The highest grades are associated with quartz-biotite-epidote veins and shears in biotite-epidote schists close to the contacts with felsic gneisses. The highest density of veins and shears commonly developed along the hanging wall contact with the tonalitic gneisses

Ekuja Dome at the base of the SZ accretionary prism and close to, or within, the subduction channel of the Pan-African subduction zone. The depletion in CaO, Na<sub>2</sub>O, and MgO most likely reflects the breakdown of plagioclase and hornblende from original amphibolite during alteration and retrogression to biotite-epidote schist (Fig. 8). The pervasive biotite alteration in mafic units is reflected in the increase in K<sub>2</sub>O recorded throughout the mineralized parts of the OSZ. The immediately surrounding tonalitic gneisses or amphibolites of the Ekuja Dome are unlikely sources for the K<sub>2</sub>O. However, the thick, quartz-biotite schist-dominated sequence of the Kuiseb Formation surrounding the Ekuja Dome seems a more likely source of K<sub>2</sub>O and possibly water during retrogression and fluid flow under upper greenschist to mid-amphibolite conditions. This would again point to the external source of the fluids, derived from surrounding rocks of the accretionary prism and, indeed, a subduction channel.

#### Constraints on the conditions and origin of ore fluids

The retrogression of amphibolites in the OSZ points to post-peak metamorphic conditions of fluid flow. While syn-deformational (D2) biotite-epidote assemblages are dominant, late-stage chlorite replacing biotite occurs in minor amounts. This emphasizes the retrogression of initially upper and middle amphibolite-facies mineral assemblages to progressively lower amphibolite- and upper greenschist-facies assemblages in the OSZ and reflects deformation during the exhumation of the rocks (Kitt et al. 2016). This agrees with the crystal-plastic

deformation and dynamic recrystallization of gneisses and mylonitization in the OSZ that points to temperature conditions of at least 450–500 °C (Passchier and Trouw 2005). The O-isotope fractionations, given not only the empirical calibration of Bottinga and Javoy (1975) but also the theoretical fractionations of Zheng (1995), provide temperatures for the quartz-biotite, quartz-feldspar, and quartz-amphibole pairs that are clearly compatible with upper greenschist- to middle amphibolite-facies conditions (temperatures of 500 to 650 °C) (ESM 5). The results show that the mineral pairs are in apparent equilibrium at these temperatures, but with quartz-biotite temperatures that are marginally lower than those for quartz-amphibole pairs. While quartz cannot be in equilibrium with both biotite and amphibole at different temperatures, the given temperatures may still approximate apparent formation temperatures as quartz is a dominant oxygen-bearing phase within the rocks. Moreover, the hydration fluid may well have been buffered by the rocks, and/or was relatively small in amount, hence close to equilibrium with the constituent minerals within the rocks. As such, no large changes in isotopic composition are to be expected as indicated by the absence of mineral-mineral reversals in terms of their order of <sup>18</sup>O enrichment, that is

$\delta^{18}\text{O}_{\text{qtz}} > \delta^{18}\text{O}_{\text{plag}} > \delta^{18}\text{O}_{\text{ep}} > \delta^{18}\text{O}_{\text{amp}} > \delta^{18}\text{O}_{\text{bt}}$ . This underlines that there was not a pervasive throughput of large volumes of externally derived fluids in the OSZ. Instead, the rather low fluid/rock ratio points to the possible local redistribution of original Cu mineralization. In fact, Steven et al. (2000) suggested only local redistribution and concentration

of Cu mineralization from an initially late Mesoproterozoic (ca. 1100 Ma) Keweenaw-type mineralization, in which the originally basaltic flows and flow-top breccias were mineralized during later Pan-African tectonism and fluid flow. This notion of an original and subsequently remobilized Cu mineralization is supported by elevated Cu values of >1500 ppm in pristine and unretrogressed regional amphibolite from the farm Barreshagen. A primary introduction of Cu mineralization during original seafloor hydrothermal alteration of a mafic volcanic sequence can also not be excluded. In fact, the somewhat elevated  $\delta^{18}\text{O}$  values of the mafic rocks (amphibolites), but good mineral-mineral equilibrium within these metamorphosed equivalents is typical of a closed-system metamorphism of seawater hydrothermally altered rocks (e.g., Putlitz et al. 2000).

The above is also compatible with the hydrogen isotope compositions of the minerals analyzed (biotite and amphibole), which also do not show any “reversals” in terms of their relative D enrichments and their range in values is typical of metamorphic-magmatic rocks. This is illustrated in the table in ESM 5, which indicates the range of calculated H- and O-isotopic compositions of waters in equilibrium with the minerals at the temperatures of equilibration (500 to 600 °C).

The homogeneous  $\delta^{34}\text{S}$  values of the chalcocite in veins, pegmatites, whole rocks (retrogressed amphibolites), and in massive ore zones between different lithotypes (ESM 6) are also compatible with a local redistribution of sulfur during metamorphism. Comparisons with other studies on metamorphosed ore deposits, such as volcanic massive sulfide deposits or even Kuroko-style mineralization, indicates that the S-isotope compositions of precursor ore mineralization is often preserved in terms of average bulk values for the sulfides (e.g., Ohmoto 1986; Large 1992). However, in contrast to typical metamorphosed volcanic massive sulfide (VMS) deposits that generally have a range in  $\delta^{34}\text{S}$  values of between 0 and 10 ‰, the range in  $\delta^{34}\text{S}$  values measured for Omitiomire is rather low at  $-4.7$  to  $-6.1$  ‰, averaging  $-5.4$  ‰. For both the VMS deposits as well as Kuroko-style deposits, the range in  $\delta^{34}\text{S}$  values is argued to be related to a complex interaction of magmatic sulfur-bearing solutions with seawater sulfate, but where the seawater is the minor constituent (e.g., Ohmoto et al. 1983; Ohmoto 1986; Large 1992). Given the large range of seawater sulfate  $\delta^{34}\text{S}$  values over geologic time, the actual range in  $\delta^{34}\text{S}$  values for different VMS deposits is also quite large and correlates with that of the seawater sulfate for the period of mineralization (Large 1992). In fact, some VMS deposits have  $\delta^{34}\text{S}$  values that extend down to an average of  $-5$  ‰ (e.g., Mt. Chalmers in Large 1992). In other cases, homogeneous  $\delta^{34}\text{S}$  values with negative values, such as measured for Omitiomire, have been noted for magmatic intrusive rocks, notably the Bushveld Igneous Complex (Liebenberg 1970), the Keweenaw Cu deposits (e.g., Donoghue et al. 2014), but also in the case of the oxide zone ores in Kuroko

deposits (Ohmoto 1986). In all such cases, an interaction with sediments and sedimentary sulfur sources, often of biogenic or diagenetic origin, are considered as explanations for the range extending towards negative  $\delta^{34}\text{S}$  values. Such interactions are clearly possible for the case of Omitiomire, where the relationship of chalcocite mineralization with epidote-biotite mineralization and the parallel enrichment in K hint at metamorphic fluids that may have been derived from the regionally metamorphosed sedimentary rocks of the Kuiseb Formation and have interacted with a pre-existing sulfide mineralization of likely magmatic origin.

### Regional correlations

Basement gneiss complexes in the SZ of the Damara Belt show remarkable similarities with Palaeo- to late Mesoproterozoic basement complexes in the Domes Region of the Lufilian Arc of Zambia, both in terms of their geochronology and tectonostratigraphic position, as well as the structural and metamorphic evolution (Unrug 1983; Kampunzu and Cailteux 1999; Porada and Berhorst 2000; Rainaud et al. 2005; Lehmann et al. 2015). With the discovery of major new Cu deposits in recent years, the Domes Region has become an important Cu district in Zambia, accounting for up to 10% of Cu resources in the Central African Copperbelt (Sillitoe et al. 2015). Unlike the world-class low metamorphic grade sedimentary-hosted stratiform deposits that characterize the Central African Copperbelt, Cu mineralization in the Domes Region is associated with high-grade, amphibolite-facies, basement inliers (Benham et al. 1976; Cosi et al. 1992; Bernau et al. 2013). Most recently, several studies on Cu mineralization in the Mwombezi Dome, Western Zambian Copperbelt, have focused on the geology and geochemistry (Bernau et al. 2013), geochronology (Sillitoe et al. 2015; Turlin et al. 2016), and petrography and microstructure (Turlin et al. 2016). These studies emphasize that the Cu mineralization occurred through the remobilization of an older (Palaeo- to late Mesoproterozoic) precursor mineralization episode that was focused into high-grade metamorphic, Pan-African (530–510 Ma) shear zones in and along granite-gneiss hosted basement sequences. Both the timing and the constrictional-type shear zones associated with Cu mineralization in the Mwombezi Dome are remarkably similar to the high-strain zones described from the OSZ in the Ekuja Dome (Bernau et al. 2013; Kitt et al. 2016). These similarities and the likely continuation of tectonostratigraphic zones from the Damara Belt through northern Botswana to the Lufilian Arc suggest a close correlation between the development of the Omitiomire deposit and the Cu deposits in the Domes Region of

Zambia, pointing to a much larger regional extent of this Cu province (Kitt et al. 2016).

## Conclusions

Cu mineralization of the Omitiomire deposit in the Southern Zone of the Pan-African Damara Belt is the result of a multi-stage evolution involving two main mineralizing events, one in the late Mesoproterozoic and one during the Pan-African. Early-stage mineralization is related to the emplacement of Cu-mineralized basaltic flows at ca. 1100 Ma. These basaltic flows were probably similar to Keweenaw-type basalts. Brecciation and dismemberment of the basaltic rocks occurred as a result of the later (ca. 1060 Ma) intrusion of mainly tonalitic melt into the previously formed basalt (stage 1 in Fig. 10). The subsequent Pan-African tectonism and subduction of the Kalahari Craton (580–520 Ma) led to the initial burial of the rocks and amphibolite-facies metamorphism of the original basalts and intrusive tonalites, but earlier intrusive contacts and the breccia-like textures between amphibolite and gneiss are still discernible in low-strain domains of the Ekuja Dome. The late-stage exhumation of the dome was associated with the expulsion of the Ekuja Dome at the base of the Southern Zone prism during northward-directed subduction. Exhumation was localized along discrete shear zones. Associated fluid flow, retrogression to middle amphibolite- to upper greenschist-facies (ca. 650–500 °C) conditions and reaction softening of original amphibolites to biotite-epidote schists led to further strain localization centered around the heterogeneous amphibolite-gneiss breccia, eventually forming the Omitiomire Shear Zone system (stage 2 in Fig. 10). Despite this, fluid/rock ratios remained low, but deformation and fluid flow led to the local redistribution of Cu into the retrograde shear zones, particularly along lithological contacts. The progressive transposition, duplication, and stacking of Pan-African structures in the shear zone system resulted in the development of linear ore shoots parallel to the pervasive north-south Pan-African stretch. There are striking similarities in the timing and polyphase evolution of the mineralization, as well as structural controls and ore body geometries at Omitiomire compared to Cu deposits in the Domes Region of the Lufilian Arc. This may suggest the existence of a much larger contiguous Cu province, with important implications for exploration.

**Acknowledgements** We are grateful to International Base Metals Limited (IBML) and Craton Mining and Exploration (Pty) Ltd. for supporting this project. Hélène Raud is acknowledged for the work done during the sampling and the many tedious hours spent separating the minerals analyzed in the stable isotope laboratory, as is the assistance of Benita Putlitz for her help in guiding Hélène through the laboratory tasks. We acknowledge the technical staff at the ICP-MS and XRF analytical facilities (CAF) in Stellenbosch. Leapfrog Africa and ARANZ Geo (Pty)

Ltd. is thanked for generously providing training and an academic license for the Leapfrog Geo 3D modeling software. We thank Karl Hartmann, Ken Maiden, Hartwig Frimmel, and Editor-in-chief Bernd Lehmann for providing constructive reviews that significantly improved the manuscript. This project relied on geological logging data from an extensive drill hole database and we acknowledge the work of the many geologists and sampling crews who worked at Omitiomire over the years, including the detailed logging done by Ken Hart.

## References

- Barnes JD, Selverstone J, Sharp ZD (2004) Interactions between serpentinite devolatilization, metasomatism and strike-slip strain localization during deep-crustal shearing in the Eastern Alps. *J Metamorph Geol* 22:283–300
- Bauer K, Vennemann TW (2014) Analytical methods for the measurement of hydrogen isotope composition and water content in clay minerals by TC/EA. *Chem Geol* 363:229–240
- Benham DG, Greig DD, Vink BW (1976) Copper occurrences of Mwombezhi Dome area, northwestern Zambia. *Econ Geol* 71: 433–442
- Bernau R, Roberts S, Richards M, Nisbet B, Boyce AJ, Nowecki J (2013) The geology and geochemistry of the Lumwana Cu ( $\pm$ Co  $\pm$  U) deposits, NW Zambia. *Mineral Deposita* 48:137–153
- Borg G, Maiden KJ (1989) The middle Proterozoic Kalahari copper belt of Namibia and Botswana. In: Boyle RW, Brown AC, Jefferson CW, Jowett EC, Kirkham RV (eds) *Sediment-hosted stratiform copper deposits*, Geol Assoc Can Spec Paper, vol 36, pp 525–540
- Bottinga Y, Javoy M (1975) Oxygen isotope partitioning among minerals in igneous and metamorphic rocks. *Rev Geophys* 13:401–418
- Cailteux JLH, Kampunzu AB, Lerouge C, Kaputo AK, Milesi JP (2005) Genesis of sediment-hosted stratiform copper–cobalt deposits, central African Copperbelt. *J Afr Earth Sci* 42:134–158
- Cosi M, de Bonis A, Gosso G, Hunziker J, Martinotti G, Moratto S, Robert JP, Ruhlman F (1992) Late Proterozoic thrust tectonics, high-pressure metamorphism and uranium mineralization in the domes area, Lufilian Arc, northwestern Zambia. *Precamb Res* 58: 215–240
- Coward MP (1981) The junction between Pan-African mobile belts in Namibia: its structural history. *Tectonophysics* 76:59–73
- Donoghue KL, Ripley EM, Li C (2014) Sulfur isotope and mineralogical studies of Ni-Cu sulfide mineralization in the bovine igneous complex intrusion, Baraga Basin, northern Michigan. *Econ Geol* 109: 325–341
- Fisher LA, Cleverley JS, Pownceby M, MacRae C (2013) 3D representation of geochemical data, the corresponding alteration and associated REE mobility at the ranger uranium deposit, Northern Territory, Australia. *Mineral Deposita* 48:947–966
- Goddard JV, Evans JP (1995) Chemical changes and fluid–rock interaction in faults of crystalline thrust sheets, northwestern Wyoming, USA. *J Struct Geol* 17:533–547
- Grant JA (1986) The isocon diagram—a simple solution to Gresen's equation for metasomatic alteration. *Econ Geol* 81:1976–1982
- Gray DR, Foster DA, Meert JG, Goscombe BD, Armstrong R, Trouw RAJ, Passchier CW (2008) A Damaran perspective on the assembly of southwestern Gondwana. *Geol Soc London Spec Publ* 294:257–278
- Gregory MJ (2006) Copper mobility in the Eastern Creek Volcanics, Mount Isa, Australia: evidence from laser ablation ICP-MS of iron-titanium oxides. *Mineral Deposita* 41:691–711
- Gresens RL (1967) Composition–volume relationships of metasomatism. *Chem Geol* 2:47–55

- Hippertt JF (1998) Breakdown of feldspar, volume gain and lateral mass transfer during mylonitization of granitoid in a low metamorphic grade shear zone. *J Struct Geol* 20:175–193
- Hitzman MW, Broughton D, Selley D, Woodhead J, Wood D, Bull S (2012) The Central African Copperbelt: diverse stratigraphic, structural, and temporal settings in the world's largest sedimentary copper district. *Soc Econ Geol Spec Publ* 16:487–514
- Hoefs J (2009) *Stable isotope geochemistry*. Springer, Berlin
- John T, Schenk V, Mezger K, Tembo F (2004) Timing and PT evolution of whiteschist metamorphism in the Lufilian Arc-Zambezi Belt orogen (Zambia): implications for the assembly of Gondwana. *J Geol* 112:71–90
- Kampunzu AB, Cailteux J (1999) Tectonic evolution of the Lufilian Arc (Central Africa Copper belt) during Neoproterozoic Pan African orogenesis. *Gondwana Res* 2:401–421
- Kasch KW (1986) Tectonic subdivision, lithostratigraphy and structural geology of the upper black Nossob River area. *Comm Geol Soc Namibia* 2:117–129
- Kasch KW (1987) Metamorphism of pelites in the upper black Nossob River area of the Damara Orogen. *Comm Geol Soc Namibia* 3:63–82
- Kitt S, Kisters A, Steven N, Maiden K, Hartmann K (2016) Shear-zone hosted copper mineralisation of the Omitiomire deposit—structural controls of fluid flow and mineralisation during subduction accretion in the Pan-African Damara Belt of Namibia. *Ore Geol Rev* 75: 1–15
- Kukla PA, Stanistreet IG (1991) The record of the Damaran Khomas Hochland accretionary prism in central Namibia: refutation of the 'ensialic' origin of a Late Proterozoic orogenic belt. *Geology* 19: 473–476
- Large RR (1992) Australian volcanic-hosted massive sulfide deposits: features, styles, and genetic model. *Econ Geol* 87:471–510
- Lehmann J, Master S, Rankin W, Milani L, Kinnaird JA, Naydenov KV, Saalman KA, Kumar M (2015) Regional aeromagnetic and stratigraphic correlations of the Kalahari Copperbelt in Namibia and Botswana. *Ore Geol Rev* 71:169–190
- Liebenberg L (1970) The sulphides in the layered sequences of the Bushveld complex. *Geol Soc South Africa Spec Publ* 1:108–207
- Maiden KJ, Hartmann K, Steven NM, Armstrong RA, (2013) The Omitiomire deposit, Namibia: Late Tectonic copper emplacement in a Neoproterozoic (Pan-African) imbricate shear system. *Ext Abstr, SGA Meeting*, 12–15 Aug 2013. Sweden, Uppsala.
- McGowan RR, Roberts S, Foster RP, Boyce AJ, Collier D (2003) Origin of the copper-cobalt deposits of the Zambian Copperbelt; an epigenetic view from Nchanga. *Geology* 31:497–500
- Meneghini F, Kisters A, Buick I, Fagereng A (2014) Fingerprints of late Neoproterozoic ridge subduction in the Pan-African Damara Belt, Namibia. *Geology* 42:903–906
- Miller RMG (1983) The Pan-African Damara Orogen of Namibia. In: *evolution of the Damara Orogen of south west Africa/Namibia*. *Geol Soc South Africa Spec Publ* 11:431–515
- Miller RMG (2008) *The geology of Namibia*. Geological Society of Namibia, Windhoek
- O'Hara K (1988) Fluid flow and volume loss during mylonitization: an origin for phyllonite in an overthrust setting, North Carolina, USA. *Tectonophysics* 156:21–36
- Ohmoto H (1986) Stable isotope geochemistry of ore deposits. In: *stable isotopes in high temperature geologic processes*. *Min Soc America Rev Min* 16:491–559
- Ohmoto H, Mizukami M, Drummond SE, Eldridge CS, Pisutha-Amund V, Lenagh TC (1983) Chemical processes of Kuroko Formation. *Econ Geol Monograph* 5:570–604
- Oliver NHS, Thomson B, Freitas-Silva FH, Holcombe RJ, Rusk B, Almeida BS, Faure K, Davidson GR, Esper EL, Guimarães PJ, Dardenne MA (2015) Local and regional mass transfer during thrusting, veining, and boudinage in the genesis of the giant shale-hosted Paracatu gold deposit, Minas Gerais, Brazil. *Econ Geol* 110: 1803–1834
- Passchier CW, Trouw RAJ (2005) *Microtectonics*. Springer, Berlin
- Porada H, Berhorst V (2000) Towards a new understanding of the Neoproterozoic-Early Paleozoic Lufilian and northern Zambezi belts in Zambia and the Democratic Republic of Congo. *J Afr Earth Sci* 30:727–771
- Putlitz B, Matthews A, Valley JW (2000) Oxygen and hydrogen isotope study of high pressure metagabbros and metabasalts (Cyclades, Greece): implications for the subduction of oceanic crust. *Contrib Mineral Petrol* 138:114–126
- Rainaud C, Master S, Armstrong RA, Phillips D, Robb LJ (2005) Monazite U–Pb dating and <sup>40</sup>Ar–<sup>39</sup>Ar thermochronology of metamorphic events in the central African Copperbelt during the Pan-African Lufilian orogeny. *J Afr Earth Sci* 42:183–199
- Rolland Y, Cox S, Boullier AM, Pennacchioni G, Mancktelow N (2003) Rare earth and trace element mobility in mid-crustal shear zones: insights from the Mont Blanc massif (Western Alps). *Earth Planet Sci Lett* 214:203–219
- Selley D, Broughton D, Scott R, Hitzman M, Bull SW, Large RR, McGoldrick PJ, Croaker M, Pollington N, Barra F, (2005) A new Look at the Geology of the Zambian Copperbelt. *Econ Geol* 100th Anniversary Vol: 965–1000.
- Sharp ZD (1990) A laser-based microanalytical method for the in-situ determination of oxygen isotope ratios of silicates and oxides. *Geochim Cosmochim Acta* 54:1353–1357
- Sharp ZD, Atudorei V, Durakiewicz T (2001) A rapid method for determination of hydrogen and oxygen isotope ratios from water and hydrous minerals. *Chem Geol* 178:197–210
- Sillitoe RH, Perello J, Garcia A (2010) Sulfide-bearing veinlets throughout the stratiform mineralization of the central African Copperbelt: temporal and genetic implications. *Econ Geol* 105:1361–1368
- Sillitoe RH, Perello J, Creaser RA, Wilton J, Dawborn T (2015) Two ages of copper mineralization in the Mwombeshi Dome, northwestern Zambia: metallogenic implications for the central African Copperbelt. *Econ Geol* 110:1917–1923
- Steven N, Armstrong R (2003) A metamorphosed Proterozoic carbonate-hosted Co-Ni-Cu deposit at Kalumbila, Kabompo Dome: the Copperbelt ore shale in northwestern Zambia. *Econ Geol* 98:893–909
- Steven NM, Armstrong RA, Smalley TI, Moore JM (2000) First geological description of a late Proterozoic (Kibaran) andesite-hosted chalcocite deposit at Omitiomire, Namibia. In: *geology and ore deposits: the Great Basin and beyond*. *Geol Soc of Nevada Symp Proc*:711–734
- Streit JE, Cox SF (1998) Fluid infiltration and volume-change during mid-crustal mylonitization of Proterozoic granite, King Island, Tasmania. *J Metamorph Geol* 16:197–212
- Turlin F, Eglinger A, Vanderhaeghe O, André-Mayer A, Poujol M, Mercadier J, Bartlett R (2016) Synmetamorphic Cu remobilization during the Pan-African orogeny: microstructural, petrological and geochronological data on the kyanite-mica schists hosting the Cu (–U) Lumwana deposit in the western Zambian Copperbelt of the Lufilian Belt. *Ore Geol Rev* 75:52–75
- Unrug R (1983) The Lufilian Arc: a microplate in the Pan-African collision zone of the Congo and the Kalahari Cratons. *Precamb Res* 21: 181–196
- Vennemann TW, Morlok A, von Engelhardt WE, Kyser TK (2001) Stable isotope composition of impact glasses from the Nördlinger Ries impact crater, Germany. *Geochim Cosmochim Acta* 65:1325–1336
- Zheng YF (1995) Oxygen isotope fractionation in magnetites: structural effect and oxygen inheritance. *Chem Geol* 121:309–316
- Zulauf G, Palm S, Petschick R, Spies O (1999) Element mobility and volumetric strain in brittle and brittle–viscous shear zones of the superdeep well KTB (Germany). *Chem Geol* 156:135–149